inorganics

MDPI

Article

A Single Biaryl Monophosphine Ligand Motif—The Multiverse of Coordination Modes

Barbara Miroslaw [1,*], Izabela Dybala [2], Radomir Jasiński [3] and Oleg M. Demchuk [4,*]

[1] Institute of Chemical Sciences, Faculty of Chemistry, Maria Curie-Skłodowska University in Lublin, 20-031 Lublin, Poland
[2] Department of Pathobiochemistry and Interdisciplinary Applications of Ion Chromatography, Medical University of Lublin, 1 Chodzki Street, 20-093 Lublin, Poland
[3] Department of Organic Chemistry and Technology, Cracow University of Technology, 31-155 Cracow, Poland
[4] Faculty of Medicine, The John Paul II Catholic University of Lublin, 1J-Konstantynów St., 20-708 Lublin, Poland
* Correspondence: barbara.miroslaw@mail.umcs.pl (B.M.); oleh.demchuk@kul.lublin.pl (O.M.D.)

Abstract: Biaryl monophosphines are important precursors to active catalysts of palladium-mediated cross-coupling reactions. The efficiency of the phosphine-based transition metal complex catalyst has its origin in the electronic structure of the complex used and the sterical hindrance created by the ligand at an active catalyst site. The aim of this paper is to shed some light on the multiverse of coordination modes of biaryl monophosphine ligands. Here, we present the analysis of the X-ray single crystal structures of palladium(II) complexes of a family of biaryl monophosphine ligands and the first crystallographic report on a related phosphine sulfide. Despite the common biaryl monophosphine ligand motif, they show diverse coordination modes (i) starting from the activation of aromatic C atoms and producing a C,P metallacycle, through (ii) the O,P chelation to Pd(II) ions with a simultaneous demethylation reaction of one of the methoxy groups, ending up with (iii) the monodentate coordination to metal cations via P atoms or (iv) via S atoms in the case of phosphine sulfide. We relate our results to the crystal structures found in the Cambridge Structural Database to show the multiverse of coordination modes in the group of biaryl monophosphine ligands.

Keywords: biaryl monophosphine ligand; Pd coordination modes; cross-coupling reactions

check for updates

Citation: Miroslaw, B.; Dybala, I.; Jasiński, R.; Demchuk, O.M. A Single Biaryl Monophosphine Ligand Motif—The Multiverse of Coordination Modes. *Inorganics* **2023**, *11*, 399. https://doi.org/10.3390/inorganics11100399

Academic Editor: Riccardo Peloso

Received: 1 August 2023
Revised: 27 September 2023
Accepted: 6 October 2023
Published: 11 October 2023

Copyright: © 2023 by the authors. Licensee MDPI, Basel, Switzerland. This article is an open access article distributed under the terms and conditions of the Creative Commons Attribution (CC BY) license (https://creativecommons.org/licenses/by/4.0/).

1. Introduction

Biaryl monophosphines are not frequently used ligands for coordination chemistry itself. However, such voluminous ligands were designed to be used in difficult cross-coupling reactions under mild and sustainable reaction conditions [1–5]. They are versatile ligands due to their steric and electronic properties, which can be fine-tuned by modifying the structure of the aryl groups [6,7]. The presence of the phosphorus (P) atom and properly located aromatic system allow these ligands to chelate transition metals (TMs), forming stable complexes in which the P–TM bond is strong and the P–C bond is weak since the formation of the last one destroys the aromaticity [1,3]. The resulting metal–ligand complexes exhibit enhanced reactivity towards the electron pair donors, which may lead to C–Hal or C–H bond activation. On the other hand, the steric hindrance caused by the voluminous substituents at the phosphorus atom in the biaryl molecular core enhances the reaction selectivity. Thus, in many types of cross-coupling reactions, such ligands promote both the oxidative addition and reductive elimination steps [8,9]. The field of biaryl monophosphine ligands has seen a significant development during recent years, including the design and synthesis of numerous derivatives with tailored catalytic properties. Such biaryl monophosphine ligands have been applied successfully in various cross-coupling reactions to facilitate carbon–carbon or carbon–heteroatom bond formation [10–12].

Palladium-catalyzed C,P cross-coupling reactions enable a simple and practical route for syntheses of various tertiary aryl-substituted phosphine derivatives. Cross-coupling reactions are at the center of interest in many industries such as pharmaceuticals, agrochemistry, or natural products [13–15]. New sustainable strategies for palladium catalysis are still required; therefore, an understanding of the coordination behavior of biaryl monophosphine ligands may be useful in designing new synthesis routes [16–18].

We report here three new crystal structures of palladium(II) complexes with biaryl monophosphine ligand MeO*Sym*-Phos (Figure 1) and its derivatives. We compare our results with a previously reported Pd(II) complex with a differently substituted biaryl fragment (Nap-Phos) [3,19] to show the changes in coordination upon changing the ligand's structure. The analyzed ligands show a wide range of coordination modes including: (i) C,P chelation with the forming of palladacycles, (ii) O,P chelation, (iii) monodentate P ligation, and (iv) monodentate S ligation. The coordination preferences of biaryl monophosphine ligands were also examined by a structural search of the Cambridge Structural Database (CSD) [20]. The aim of this paper is to present the multiverse of coordination modes of biaryl monophosphine-based ligands.

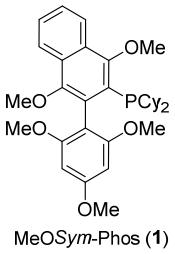

Figure 1. Structure of the MeO*Sym*-Phos ligand.

2. Results

The MeO*Sym*-Phos ligand (**1**) was obtained from inexpensive starting materials by a synthetic protocol similar to that reported previously [2]. The phosphine sulfide MeO*Sym*-PhosS (**5**) was next subjected to a desulfuration reaction by treatment with Ni-Raney reagent [21] to give ligand **1** in an almost quantitative yield (Scheme 1).

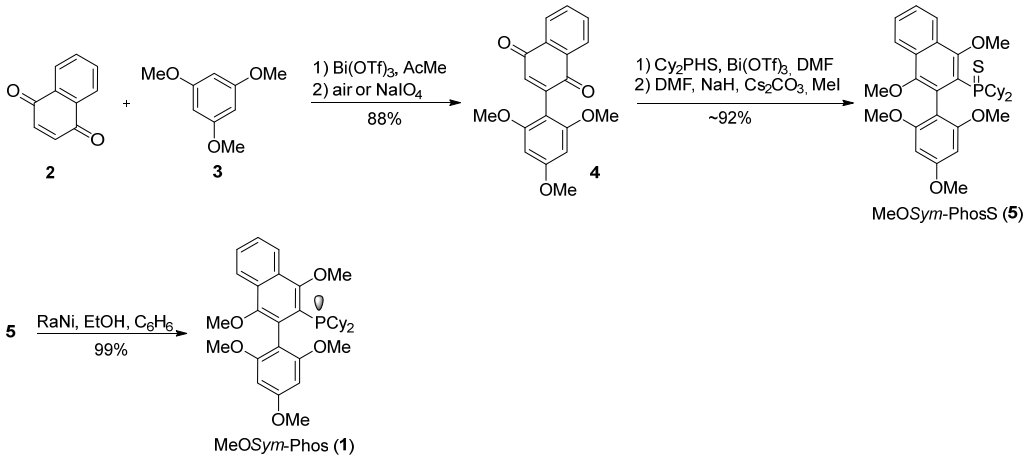

Scheme 1. Synthesis of the MeO*Sym*-Phos ligand.

Alternatively, the same ligand could be obtained through the reduction of a corresponding phosphine oxide MeO*Sym*-PhosO. The several-step reduction protocol is as follows: deoxodichlorination with $COCl_2$ followed by the reduction of phosphonium salt with LAH or reduction via $LiBH_4$ treatment to form phosphine borane and deprotection of the phosphorus atom through hydrazine treatment (Scheme 2). The typical reduction reagents ($HSiCl_3$, $PhSiH_3$, and TMDS/$Ti(OBu)_4$) were ineffective.

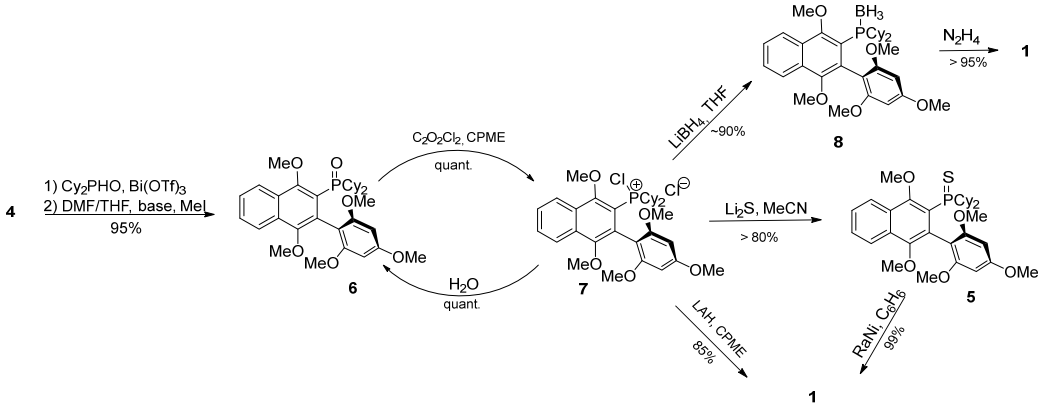

Scheme 2. The alternative route to the MeO*Sym*-Phos ligand.

The MeO*Sym*-Phos ligand presented here has a special coordination feature. The treatment of **1** with dichloropalladium complex Pd(^{t}-BuCN)$_2$Cl$_2$, at a relatively low temperature (35 °C) in acetonitrile, according to our assumptions leads to complex **9**. The Pd(II) cation activates the aromatic C atom from 1,3,5-trimethoxybenzene to bind it directly. This behavior is similar to other C,P ligands. Nevertheless, in poorly coordinating dichloromethane, the obtained complex is unstable and in the presence of an excess amount of the ligand, at a slightly higher temperature (40 °C), complex **9** is no longer formed as the main product. Instead, demethylation of one of the methoxy groups in the 1,4-dimethoxynaphthalene fragment occurs. This transformation leads to complexes **10** and **11** instead, which constitute a very interesting material to study the diversity of the coordination modes of biaryl monophosphine-based ligands (Scheme 3).

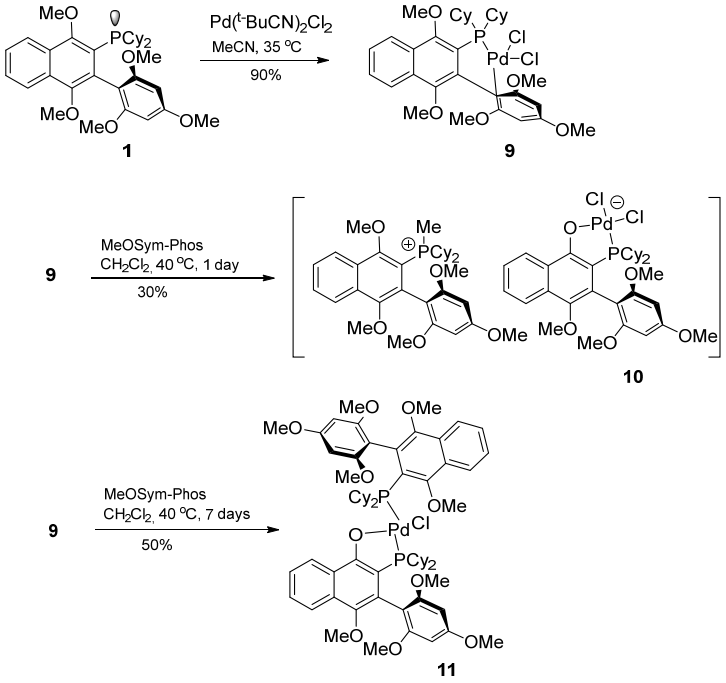

Scheme 3. Synthesis of phosphine palladium complexes **9**–**11**.

We managed to isolate as single crystals and characterize the complexes of demethylated product **10** and its derivative **11**. In the case of **10** and **11**, instead of C,P coordination, O,P chelation to Pd(II) is observed (Scheme 3). Additionally, in the crystal of **11**, the other biaryl monophosphine ligand is ligated monodentately via the P atom.

A monodentate coordination mode is also present in a sulfide derivative MeO*Sym*-PhosS (**5**), via an S atom, however. Such a complex was isolated from the reaction of **5** with

the Pd(II) source run for 40 min in dichloromethane at 40 °C. Two ligand molecules formed a typical monodentate ligand dimer bridged by halogen atoms (Scheme 4).

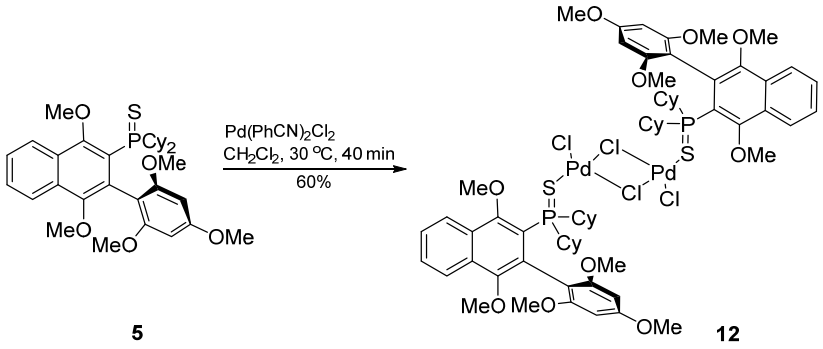

Scheme 4. Synthesis of phosphine sulfide palladium complex **5**.

It is interesting that such coordination diversity tuned by the synthesis conditions was not observed in the case of our previously studied biaryl monophosphine ligand Nap-Phos [3,19]. The palladium complex of Nap–Phos (**13**) was obtained with the utilization of tris(acetonitrile)chloropalladium tetrafluoroborate [22]. The *ortho*-substituted methoxy groups in the complex of **14** limited the free rotation around the biaryl junction and prevented the formation of a palladacycle. The Pd(II) cation linked the biaryl monophosphine ligand only via the P atom supplementing the coordination sphere by small solvent molecules and a Cl^- anion (Scheme 5). No other coordination modes were observed in the case of this ligand.

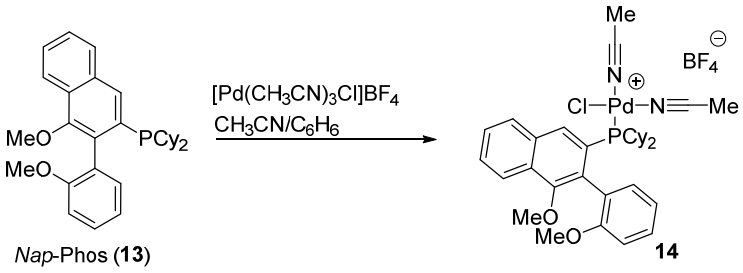

Scheme 5. Synthesis of phosphine palladium complex **14**.

2.1. Analysis of Crystalographic Data Recorded for Single Crystals of **9–12**

The single crystals for complexes **9–12** were studied by the X-ray diffraction method. A summary of the conditions for data collection and the crystal structure refinement parameters are given in Table 1. The geometry of the inter- and intramolecular interactions of structures **9–12** is given in Table 2. Crystallographic data for **9–12** have been deposited at the Cambridge Crystallographic Data Centre: CCDC 2278031-2278034. These data can be obtained free of charge via https://www.ccdc.cam.ac.uk/structures/or (accessed on 29 July 2023) by contacting the Cambridge Crystallographic Data Centre, 12, Union Road, Cambridge CB2 1EZ, UK.

Table 1. Crystal data and structure refinement for complexes **9**–**12**.

Identification Code	9	10	11	12
Empirical formula	$C_{71}H_{98}Cl_6O_{11}P_2Pd_2$	$C_{66}H_{86}Cl_2O_{10}P_2Pd$	$C_{65}H_{87}ClO_{12}P_2Pd$	$C_{87}H_{110}Cl_4O_{10}P_2Pd_2S_2$
Formula weight	1615.06	1278.68	1264.14	1796.41
Temperature/K	120	290	290	100
Crystal system	monoclinic	monoclinic	triclinic	orthorhombic
Space group	*C*2/*c*	$P2_1$	*P*-1	*Pbca*

Table 1. *Cont.*

Identification Code	9	10	11	12
a/Å	18.4535(2)	11.6734(16)	12.263(1)	22.926(5)
b/Å	15.1832(1)	17.0922(19)	13.884(1)	12.246(2)
c/Å	26.2221(2)	16.7564(19)	20.773(1)	29.303(6)
α/°	90	90	88.53(1)	90
β/°	97.482(1)	107.391(14)	85.29(1)	90
γ/°	90	90	65.98(1)	90
Volume/Å^3	7284.44(11)	3190.5(7)	3219.5(5)	8227(3)
Z	4	2	2	4
ρ_{calc}g/cm^3	1.4725	1.3309	1.304	1.450
μ/mm^{-1}	6.886	0.481	0.438	0.715
F(000)	3364.6	1343.6	1332.0	3736.0
Crystal size/mm^3	0.12 × 0.08 × 0.02	0.35 × 0.15 × 0.15	0.3 × 0.15 × 0.08	0.35 × 0.2 × 0.08
Radiation	Cu Kα (λ = 1.54184)	Mo Kα (λ = 0.71073)	Mo Kα (λ = 0.71073)	Mo Kα (λ = 0.71073)
2Θ range for data collection/°	6.8 to 135.36	5.4 to 50.48	5.16 to 50.48	4.68 to 50.48
Index ranges	$-22 \leq h \leq 22$, $-18 \leq k \leq 18$, $-28 \leq l \leq 31$	$-13 \leq h \leq 14$, $-20 \leq k \leq 20$, $-20 \leq l \leq 20$	$-14 \leq h \leq 14$, $-16 \leq k \leq 16$, $-24 \leq l \leq 24$	$-16 \leq h \leq 27$, $-14 \leq k \leq 9$, $-35 \leq l \leq 32$
Reflections collected	38,734	20,908	38,607	29,292
Independent reflections	6599 [R_{int} = 0.0408, R_{sigma} = 0.0261]	7543 [R_{int} = 0.0728, R_{sigma} = 0.1356]	11639 [R_{int} = 0.0963, R_{sigma} = 0.1492]	7433 [R_{int} = 0.1199, R_{sigma} = 0.2016]
Data/restraints/parameters	6599/0/428	7543/0/730	11,639/0/720	7433/7/427
Goodness-of-fit on F^2	1.05	0.971	1.302	0.825
Final R indexes [I>=2σ (I)]	R_1 = 0.0354 wR_2 = 0.0792	R_1 = 0.0595 wR_2 = 0.1138	R_1 = 0.0911 wR_2 = 0.2315	R_1 = 0.0513 wR_2 = 0.1236
Final R indexes [all data]	R_1 = 0.0389 wR_2 = 0.0819	R_1 = 0.0595 wR_2 = 0.1138	R_1 = 0.1509 wR_2 = 0.2502	R_1 = 0.1307 wR_2 = 0.1691
Largest diff. peak/hole/e Å^{-3}	1.48/−0.93	1.27/−0.65	1.64/−1.98	1.17/−1.22
Flack parameter	–	−0.03(3)	–	–
CCDC No.	2278033	2278034	2278032	2278031

Table 2. Geometry of intra- and intermolecular interactions in the crystals of complexes **9**–**12** [Å, °].

Complex	D-H...A	D-H	D...A	H...A	<D-H...A
9	C25-H25A...O4 [i]	0.97	3.263(4)	2.641(4)	122(1)
	C6-H6...Cl2 [ii]	0.93	3.521(3)	2.716(3)	145(1)
10	C38-H38...O9 [iii]	0.93	3.46(1)	2.67	143(1)
	C43-H43A...O1	0.96	3.41(1)	2.65	136(1)
	C47-H47...O2 [iv]	0.93	3.55(1)	2.63	170(1)
11	C44-H44B...Pd1	0.96	3.36(1)	2.73	124(1)
	C62-H62B...Pd1	0.97	3.20(1)	2.54	126(1)
	C21-H21B...O5 [v]	0.96	3.456(18)	2.65	142(1)
	C40-H40...O4 [v]	0.93	3.375(16)	2.56	147(1)
12	C27-H27A...Pd1	1.00	3.322(7)	2.42	152(2)
	C21-H21A...O1 [vi]	0.98	3.444(10)	2.63	141(1)
	C8-H8...O5 [vii]	0.95	3.492(9)	2.62	153(1)
	C7-H7...O2 [vii]	0.95	3.354(9)	2.75	122(1)
	C40-H40B...O4 [viii]	0.98	3.605(14)	2.74	148(1)
	C40-H40A...Pd1	0.98	3.712(14)	2.81	153(1)

Symmetry codes: (i) 1 − x,1 − y,1 − z; (ii) x, 1 − y, 1/2 + z; (iii) x − 1, y, z; (iv) 2 − x, 1/2+−y, −z; (v) −x + 1, −y + 1, −z; (vi) −x + 1/2 + 1, +y + 1/2, +z; (vii) −x + 1/2 + 1, +y − 1/2, +z; (viii) −x + 1, −y + 1, −z.

2.1.1. C,P Chelation in Five-Membered Palladacycle **9**

Complex **9** crystallizes in a *C*2/*c* monoclinic space group as a solvate of diethyl ether and dichloromethane. The phosphine molecule acts as a C,P chelating ligand forming a five-membered metallacycle as presented in Figure 2, with the Pd1-C13 distance being 2.199(3) Å. The coordination sphere of the Pd(II) cation is supplemented by two chloride anions. The square coordination polyhedron is only slightly distorted from planarity. The

hybridization of the C13 atom in the complex changes from sp^2 to sp^3, perturbing the aromaticity of this system.

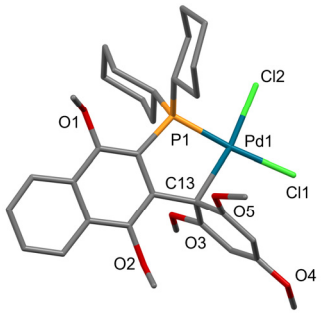

Figure 2. Structure of **9**—C,P chelation resulting in a five-membered palladacycle (hydrogen atoms and solvent molecules were omitted for clarity).

2.1.2. O,P Chelation with Simultaneous Demethylation to Form Five-Membered Palladacycle **10**

The crystal structure of **10** (chiral space group $P2_1$) is a salt composed of a methylphosphonium cation and an anionic complex of Pd(II) (Figure 3). The proximity of the palladium atom, which is a p-electron acceptor, enhances the electrophilicity of the methoxy group located at the *ortho*- to phosphorus atom position. Because of this, the MeO*Sym*-Phos ligand present in excess in the reaction mixture undergoes P-methylation. As a result, an anionic complex is formed in which Pd(II) coordinates to O and P atoms. The $-CH_3$ group is transferred to the phosphine molecule, forming a phosphonium cation (Figure 3). Similar to structure **9**, the coordination sphere of Pd(II) is supplemented by two Cl^- anions.

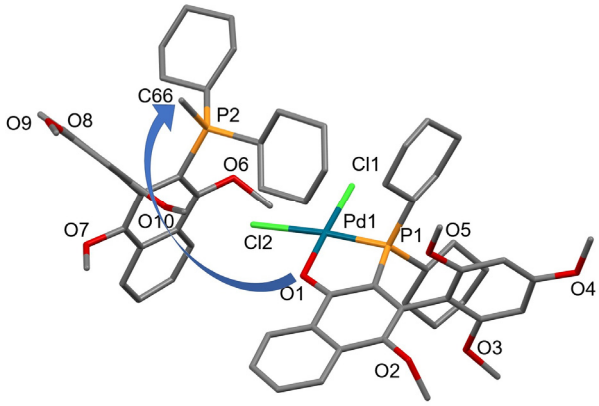

Figure 3. Structure of **10**—O,P chelation to the Pd(II) ion with simultaneous P-methylation (hydrogen atoms and solvent molecules were omitted for clarity).

2.1.3. Additional Monodentate P Ligation by Five-Membered Palladacycle **11**

The chloride anions in the palladium(II) coordination sphere showed themselves to be quite easily replaced with other ligands, for example, by an additional molecule of the phosphorus ligand. In such a way, electrically neutral complex **11** was formed. **11** crystallizes in a centrosymmetric space group *P*-1. The charge of the planarly tetracoordinated Pd(II) cation is neutralized by one chloride anion and deprotonated at the O1 atom phosphine ligand. The demethylated organic ligand forms an *O,P* coordinated chelate similar to **10** and a second molecule of MeO*Sym*-Phos binds palladium(II) as a monodetate ligand through the P atom (Figure 4). Two phosphorus centers in the coordination sphere are in *trans* positions following the trans rule. It is worth noticing that the two large phosphine ligands are arranged mutually in a head-to-head fashion with voluminous cyclohexyl groups turned in the same direction. This spatial arrangement favors an intramolecular agostic interaction [23] between Pd1 and the H44B atom from a methoxy group of the

non-demethylated phosphine ligand (d(Pd1...C44) = 3.36(1) Å) (Table 2). It may be regarded as a preactivation stage of the demethylation reaction. The agostic interactions have been proven to play an important role in many transition metal complexes and in catalytic chemical reactions [24–29].

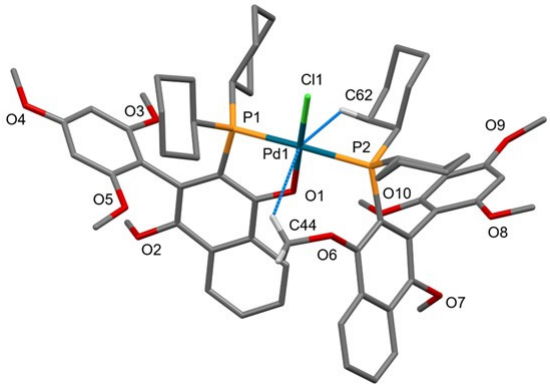

Figure 4. Structure of **11**—monodentate P ligation and O,P chelation to the Pd(II) ion with two C–H...Pd contacts (blue dashed lines).

2.1.4. Monodentate S ligation of Biaryl Monophosphine Sulfide **12**

The outstanding basicity of a phosphorus atom in MeO*Sym*-Phos enhances the nucleophilicity of a sulfur atom of the corresponding phosphine sulfide MeO*Sym*-PhosS (**5**) and contributes to efficient palladium coordination. This is the first report on the crystal structure of a palladium(II) coordination compound of a biaryl monophosphine sulfide. The crystal of **12** is a toluene solvate (orthorhombic space group *Pbca*). Only half of the molecule is symmetrically independent (Z′ = 0.5). One of the solvent molecules occupies a special position in the center of inversion. The phosphine sulfide used in **11** as a ligand binds monodentately via the S atom only. However, the coordination sphere of Pd(II) is supplemented by three Cl^- anions, forming a planar dinuclear core with two chloride bridges (Figure 5). The space below and above each metal ion is occupied by two H atoms. One of the C–H groups in the cyclohexyl substituent interacts with the metal center by forming a directional interaction that can be regarded as an agostic one, with the C27...Pd1 distance being 3.322(7) Å (Table 2). From the other side, the methyl group of toluene approaches the metal center but with a longer distance of 3.712(14) Å.

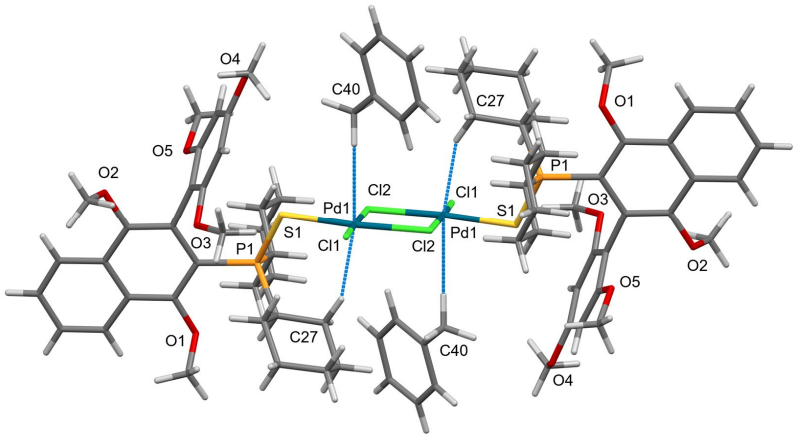

Figure 5. Structure of the complex of MeO*Sym*-PhosS **12** (the C–H...Pd contacts are presented as blue dashed lines).

2.1.5. Monodentate P Ligation of Nap-Phos in **14** with Unusual C–H...Pd Contacts

14 crystallizes as a cationic complex in an orthorhombic space group $P2_12_12_1$ with two symmetrically independent molecules in the unit cell, and BF_4 ions neutralize the

electric charge [3,19,22]. The coordination sphere of the Pd(II) ion is composed of a monodentate P-ligating phosphorous ligand, one chloride anion, and two acetonitrile molecules (Figure 6). The biaryl monophosphine ligand has only two methoxy groups substituted in the *ortho*-position regarding the aryl–aryl bond. This creates a rotation barrier; however, the steric hindrance is smaller than in the MeO*Sym*-Phos ligand. It is interesting that, analogously to the structure of complex **12**, here, the Pd(II) ion is also surrounded by two C–H contacts, with one coming from the cyclohexyl substituent (with the C30. . .Pd1 distance being 3.33(1) Å), and the other even shorter (with the C12. . .Pd1 distance being 2.93(1) Å) coming from the aromatic ring. This may suggest that this complex tends to undergo an intramolecular C–H activation reaction leading to the six-membered palladacyclic complex (see Section *Six-Membered Palladacycles*) more willingly than to interact with the π-electron density of the aromatic methoxyphenyl moiety [3].

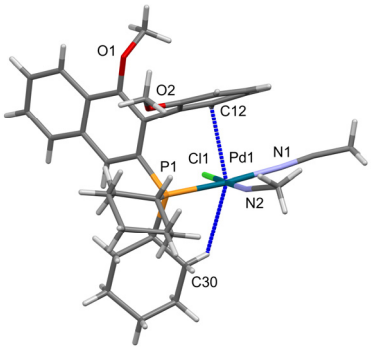

Figure 6. Structure of **14** (the C–H. . .Pd contacts presented as blue dashed lines) (CSD Refcode XISCEJ01) [22].

2.2. Multiverse of Coordination Modes of Biaryl Monophosphine Ligands Based on the CSD Survey

To gain a broader view of the coordination preferences of biaryl monophosphine ligands in coordination with palladium, a search in the CSD (ver. 5.43 with updates) was performed [20]. It gave 277 hits of palladium complexes with biaryl monophosphine derivatives. The particular coordination modes are discussed below. One remark should be made here before the discussion. According to the IUPAC regulations, the term metallacycle should be used for a strictly defined group of compounds [30,31]. However, there are many examples in the literature where this term is used in a "wider sense" to describe the analyzed cyclic coordination compounds regardless of their bonding type [32–34]. Such interpretation is used in the present discussion.

2.2.1. C,P Chelation—Four- and Five-Membered Metallacycles

The activation of the C atom is one of the characteristic features of Pd. The four-, five-, or six-membered metallacycles involving the coordination via the phosphine P atom with simultaneous formation of a direct C–Pd bond are of great importance in transition metal-catalyzed cross-coupling reactions. In the CSD, there are reports on only 8 four-membered and 8 five-membered palladacycles, and 62 hits for six-membered ones. A structural characterization of some examples is presented below.

Four-Membered Palladacycles

Four-membered palladacycles are rare, and they are usually formed in the way of an *ortho*-palladation reaction [35]. The phosphorus-containing palladacycles have been observed in only eight structures. Five of them were previously mentioned dimeric species doubly bridged by chloride ions, one was bridged by an acetate anion, whereas two of them were mononuclear, supplementing the metal coordination sphere by acetonitrile or trifluoroacetate molecules. As for their application, Montgomery et al., for example, re-

ported the great performance of the palladium(II) complex with *ortho*-biphenyl phosphines S-Phos with the acetate bridge (Figure 7) CSD Refcode NIXTIA) [36].

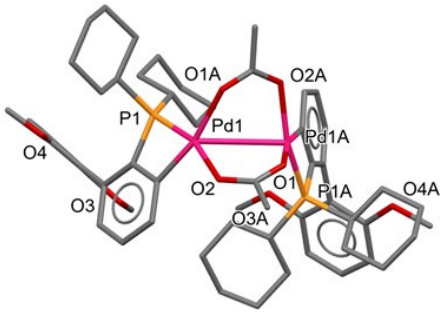

Figure 7. Four-membered palladacyclic complex of S-Phos (CSD Refcode NIXTIA) [36].

Allgeier et al. reported the X-ray structures of such a four-membered palladacyclic complex of the tBuXPhos catalyst (Figure 8) (CSD Refcode ZEJKEG) [37] and the products of its degradation.

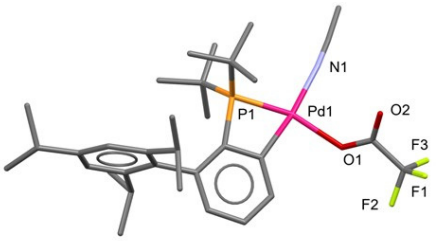

Figure 8. Monomeric four-membered palladacyclic complex of tBuXPhos (CSD Refcode ZEJKEG) [37].

The four-membered ring formation has also been reported by Christmann et al. (Figure 9) (CSD Refcode REHPEA) [38]. They studied a catalytic amination of aryl chlorides. The formation of strained four-membered Pd(II) cyclometallates was reported to depend on the nature of the phosphine substituents and the kind of halides used, which tend to bridge the four-membered palladacycles in dimeric units.

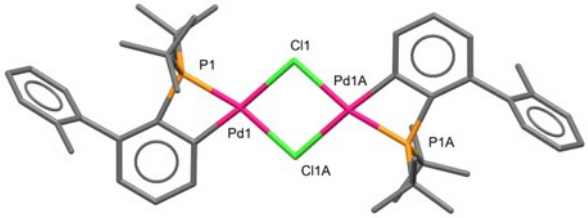

Figure 9. Dimeric four-membered dichloropalladacyclic complex of P*t*Bu2(Bph-Me) (CSD Refcode REHPEA) [38].

An analogous μ-chloro Pd(II) dimer was characterized by Toriumi et al. (Figure 10) (CSD Refcode EBEFAW) [39]. They studied the mechanism of the visible light-induced carboxylation of aryl halides and triflates. The obtained complex was a by-product in the course of the synthesis of the desired photoredox catalyst, but instead, the C–H activation reaction yielded the four-membered dichloropalladacyclic complex.

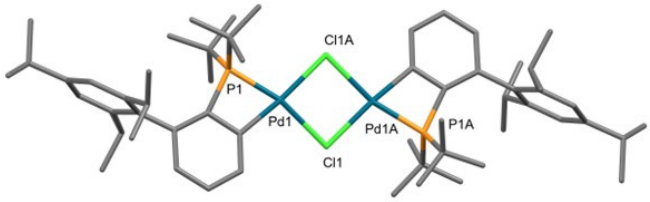

Figure 10. Dimeric four-membered dichloropalladacyclic complex of tBuXPhos (CSD Refcode EBEFAW) [39].

Five-Membered Palladacycles

Five-membered palladium metallacycles are more widespread than the four-membered ones. There are 62 hits for such molecular architecture in the CSD and their geometry is very similar. An interesting example was presented by Lalloo et al. where the authors discussed the decarbonylative fluoroalkylation process (Figure 11) (CSD Refcode JAKQOF) [40]. Based on their findings one may conclude that the Pd(II) ion is responsible for the C–H activation within the aromatic biphenyl part. Additionally, the metal core may also affect the transmetalation reaction by enhancing the F_2C–H. . .X intramolecular interaction. The carbonyl de-insertion reaction was slow for X = difluoroacetate where no F_2C–H. . .X contacts were found but fast with X = F, where a hydrogen bond could be formed.

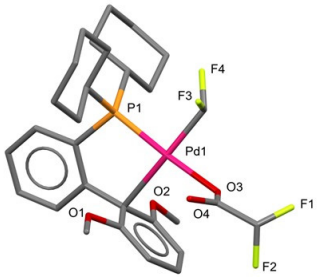

Figure 11. An example of the five-membered palladium metallacyclic complex of S-Phos (CSD Refcode JAKQOF) [40].

Six-Membered Palladacycles

Six-membered metallacycles similar to the four-membered ones are not frequent. Among the 277 biaryl monophosphine Pd complexes, there are only nine hits. An example may be the cyclopalladated biaryl derivative reported by Pratap et al. during studies on aryl amination and C−C bond-forming reactions (Figure 12) (CSD Refcode WULGOA) [41]. The 2-(dicyclohexylphosphino)biphenyl was proven to catalyze the C−C bond formation, but it was ineffective in the aryl amination of nucleosides.

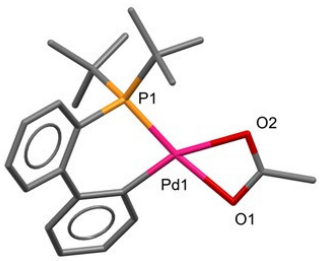

Figure 12. A representative example of six-membered metallacyclic complexes (CSD Refcode WULGOA) [41].

2.2.2. Chelation via Heteroatoms Forming Seven-Membered Rings

The substitution at the 2,2′-positions in a biaryl moiety offers the possibility to form seven-membered rings, including ligation through the phosphine P atom and an additional C, N, O, or S atom coming from the proper substituent. However, there are only eight

structures in the CSD with such molecular architecture. An example of the practical use of a seven-membered ring arrangement was demonstrated by Buchwald et al. for the synthesis of biaryl amides with axial chirality (Figure 13) (CSD Refcode XUZWIZ) [42]. They showed that the stereoselectivity in this case was supported not only by the steric hindrance caused by the aryl molecular fragments but the weak C–H. . .O interactions also made their own contribution to the C−C coupling reaction.

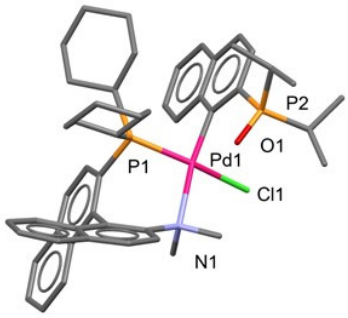

Figure 13. A seven-membered metallacyclic complex of KenPhos (CSD Refcode XUZWIZ) [42].

A seven-membered ring with P,O coordination was present in a complex being an intermediate state in a decarbonylative cross-coupling process which was reported to run easily at room temperature (Figure 14) (CSD Refcode GOCLES) [43]. The advantage of this complex is the weak O(isopropoxy)–Pd linkage, which may break easily in the presence of $(DMPU)_2Zn(CF_2H)_2$ (where the DMPU is *N*,*N*′-dimethylpropyleneurea). The formed empty coordination site is prone to accept a carbonyl ligand. However, the authors emphasize that the chloro complex is quite stable itself. It does not undergo any decarbonylation up to 120 °C, but once the Cl ligand is replaced by the difluoromethyl one, decarbonylation runs rapidly even below room temperature (7 °C). It seems once again that the weak F_2C–H. . .*X* interactions may favor the palladium-catalyzed cross-coupling reactions.

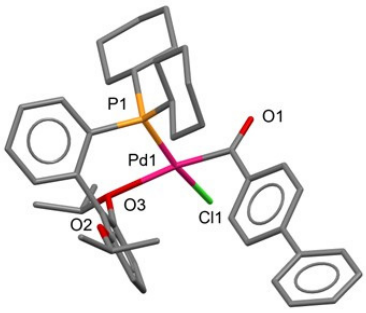

Figure 14. A representative seven-membered metallacyclic complex of RuPhos (CSD Refcode GOCLES) [43].

2.2.3. Monodentate P Ligation

The simplest monodentate ligation by only the P atom was found in nearly half of all structures (112 hits). This type of ligation is possible when the Pd coordination sphere is preoccupied with other strongly binding ligands, usually chelating ones. Such a type of complex was described by Bruno et al. during their studies on a new palladium mesylate precatalyst for C–C and C–N cross-coupling reactions (Figure 15) (CSD Refcode WETDAC) [44]. They proposed a hypothesis that it would be possible to incorporate larger ligands into the Pd(II) coordination sphere by increasing the electron deficiency of the metal center. They managed to do so in the course of replacing the chloride with a more electron-withdrawing mesylate anion. The complexes shown in Figure 15 with chloride and mesylate anions do not differ significantly in geometry. However, the mesylate anion proved to be more labile in a chloroform solution which was confirmed by ^{31}P NMR spectroscopy.

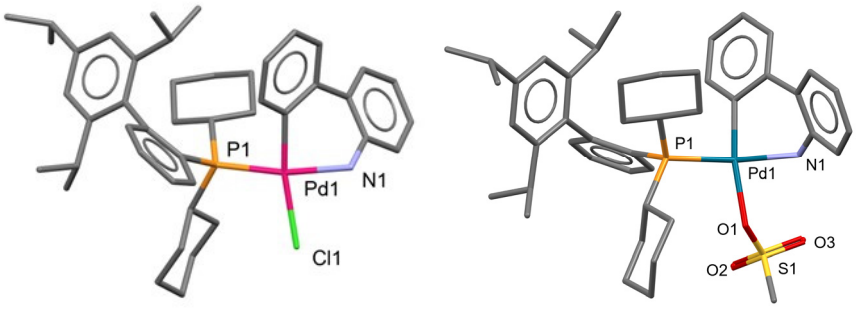

Figure 15. Representative examples of the monodentate coordination of palladium by a biaryl monophosphine ligand *t*BuXPhos (CSD Refcodes WETDAC—**left** and WETDOQ—**right**) [44].

One of the interesting features of monodentate P ligation is that it may result in the formation of dinuclear palladium cores bridged by various linkers such as halogen atoms, OH ions, or even larger molecules like 4-methylaniline (32 hits). Such a molecular arrangement was found in a group of halogen-bridged dinuclear palladium precatalysts used in selected coupling reactions [45]. It is also considered as the first intermediate stage in the cross-coupling reaction catalytic cycle—the oxidative addition step [9]. An interesting chloride bridged structure was presented by Biscoe et al. in studies on the catalytic selectivity of biaryl monophosphine ligands (Figure 16) (CSD Refcode JIMMEY) [46]. They focused on the role of the electronic properties of amines and their acidity in catalytic arylation reaction selectivity.

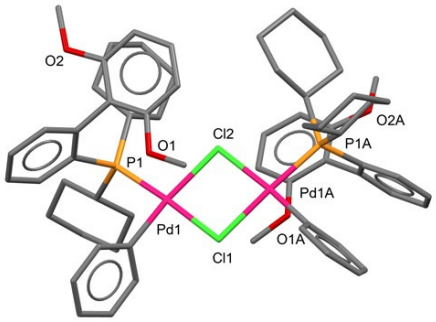

Figure 16. Dinuclear palladium complex of S-Phos as a monodentate ligand (CSD Refcode JIMMEY) [46].

2.3. Coordination Modef of Phosphine Sulfides

There is no report in the CSD on any crystal structure of a palladium complex with a biaryl monophosphine sulfide; our report is the first one. Such catalysts are less frequently studied. However, we can compare our results with five hits containing palladium complexes of biaryl biphosphine sulfide derivatives studied by Faller and Wilt in the search for a catalyst for asymmetric allylic amination [47]. The coordination motive was chelation via P and S atoms, as shown in Figure 17 (CSD Refcode LAYWIS) [48]. The sulfur atom was incorporated into the eight-membered palladacycle. The remaining coordination sites of palladium were filled with two chloride anions or dienyl derivatives, forming η^3 coordination compounds. The catalysts showed high regioselectivity in the asymmetric allylic amination of acyclic allylic carbonates.

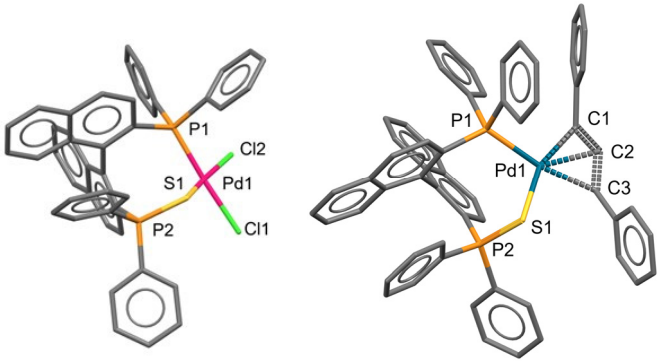

Figure 17. Eight-membered metallacyclic complexes of BINAP mono-sulfide (CSD Refcodes LAYWIS—**left** and LAYWOY—**right**) [48].

3. Materials and Methods

3.1. Chemistry

The reagents were purchased from commercial suppliers and used without further purification. The solvents were dried and distilled under argon before use. All of the reactions involving the formation and further conversion of phosphines were carried out under argon atmosphere with the attempted complete exclusion of air from the reaction vessels and solvents, including those used in the work-up. Nuclear magnetic resonance (NMR) spectra were recorded on Bruker AV300 (^{1}H 300 MHz, ^{31}P 121.5 MHz, and ^{13}C NMR 75 MHz) and Bruker AV500 (^{1}H 500 MHz, ^{31}P 202 MHz, and ^{13}C NMR 126 MHz) spectrometers (Bruker; Billerica, MA, USA). All spectra were obtained in $CDCl_3$ solutions unless mentioned otherwise, and the chemical shifts (δ) are expressed in ppm using internal reference to TMS and external reference to 85% H_3PO_4 in D_2O for ^{31}P. Coupling constants (J) are given in Hz. The abbreviations of signal patterns are as follows: s—singlet, d—doublet, t—triplet, q—quartet, m—multiplet, b—broad, and i—intense. Thin-layer chromatography (TLC) was carried out on silica gel (Kieselgel 60, F254 on an aluminum sheet, Merck, Rahway, NJ, USA). All separations and purifications by column chromatography were conducted by using Merck Silica gel 60 (230–400 mesh) unless noted otherwise. HPLC-MS spectra were performed in methanol using high-performance liquid chromatograph Agilent 1200 conjugated with Agilent 6120 or Agilent 6538 UHD Accurate-Mass Q-TOF spectrometers (Agilent Technologies, Inc., Santa Clara, CA, USA). For separation, a stationary flow of acetonitrile/water was applied, with a rate of 0.3 mL/min on a ReproSil-Pur Basic-C18, 3 µm, 100 × 2 mm column (Dr. Maisch, High Performance LC GmbH, Ammerbuch-Entringen, Germany) at 23 °C. Electrospray ionization (ESI) was applied, and the data were acquired in positive and negative ion modes.

The phosphine sulfide **5** was obtained in a similar manner to that published in [2]: the oxide of dicyclohexylphosphine was replaced in this case by dicyclohexylphosphine sulfide. And phosphine **1** was obtained according to the desulfuration protocol presented in [21].

Alternatively, **1** was obtained starting with its oxide **6** [2], and then treated with oxalyl chloride, which afforded the phosphonium salt **7**. Last, it could be transformed: (a) to **5** in the reaction with lithium sulfide or (b) to **1** in the reaction with $LiAlH_4$ or (c) to phosphine borane **8** in the reaction with $LiBH_4$.

3.1.1. Synthesis of Dicyclohexyl[1,4-dimethoxy-3-(2,4,6-trimethoxyphenyl)naphthalen-2-yl] phosphane sulfide (**5**)

Approximately 1.1. g (4.8 mmol) of dicyclohexylphosphine sulfide (obtained as described [49]), 1.1 g (3.4 mmol) of **4** (obtained as described [2]), and 50 mg (2 mol%) of bismuth(III) trifluoromethanesulfonate were added to 20 mL of DMF. The vial was sealed with a glass stopper and the reaction mixture was stirred for 24 h at 90 °C. After that time, the reaction mixture was cooled down to 10 °C. Next, 1.8 g (5.5 mmol) of cesium carbonate,

0.5 g (12.5 mmol) of 60% sodium hydride, and 100 mg (8 mol%) of tetrabutylammonium hydrogen sulfate were added to the reaction vessel. The mixture was stirred and protected with a slow flow of argon as long as hydrogen liberation occurred. Subsequently, 1.5 mL (24 mol) of iodomethane was added, and the vial was sealed with a glass stopper, secured with a metal clamp, and stirred for 24 h at 30 °C. Next, 100 mL of cold water was added, the crude product was extracted with dichloromethane 3 × 20 mL, the organic phase was separated and dried by magnesium sulfate, and product **5** was isolated by chromatography on a SiO_2 column using the hexane/acetone = 6/1 to 3/1 solvent mixtures to elute the substances. Yield 1.8 g (92%). HPLC-MS (CH_3CN/H_2O = 65/35, 0.3 mL/min, rf 17.2 min): measured 583.26 Da (71%), 584.26 Da (28%) [$C_{33}H_{43}O_5PS^+H^+$], calculated 583.26 Da and 583.27 Da; ^{1}H NMR (500 MHz, $CDCl_3$): 8.12 (m, 2H), 7.56 (m, 2H), 6.16 (s, 2H), 4.13 (s, 3H), 3.88 (s, 3H), 3.65 (s, 6H), 3.57 (s, 3H), 2.68 (tdt, J = 11.3, 11.3, 7.6, 3.7, 3.7, 2H), 1.62 (m. 16H), 1.3 (m, 4H), 1.19 (m, 4H), 0.86 (m, 4H); ^{13}C NMR (126 MHz, dept 135, $CDCl_3$): 127.17, 125.72, 123.73, 123.56, 90.08, 62.83, 61.10, 55.33, 55.14, 41.23, 40.83, 27.68, 27.67, 27.12, 27.11, 26.93, 26.86, 26.75, 26.55, 26.43, 25.83, 25.82; ^{31}P NMR (202 MHz, $CDCl_3$): 66.3.

3.1.2. Synthesis of Dicyclohexyl[1,4-dimethoxy-3-(2,4,6-trimethoxyphenyl)naphthalen-2-yl] phosphane (**1**)

To a mixture of 5 g of Ni-Raney and 10 mL of ethanol, a solution of 750 mg of **5** in 50 mL of benzene was added. The air in the vessel was replaced with argon. The vessel was sealed with a glass stopper, and the reaction mixture was stirred at ambient temperature for 16 h. The Ni-Raney reagent was removed by filtration, and the solvent was evaporated under reduced pressure to give phosphine **1** in 99% yield (700 mg). HPLC-MS (CH_3CN/H_2O = 80/20, 0.3 mL/min, rf 2.9 min): measured 551.29 Da (75%), 552.30 Da (35%) [$C_{33}H_{43}O_5P^+H^+$], calculated 551.29 Da and 552.30 Da; ^{1}H NMR (500 MHz, C_6D_6): 8.27 (d, J = 7.6 Hz, 1H), 8.01 (d, J = 7.6 Hz, 1H), 7.26 (m, 2H), 6.25 (s, 2H), 3.71 (s, 3H), 3.62 (s, 3H), 3.43 (s, 6H), 3.39 (s, 6H), 2.29 (m, 2H), 2.05 (m. 2H), 1.86 (m, 2H), 1.74 (m, 2H), 1.67 (m, 4H), 1.28 (m, 10H); ^{13}C NMR (126 MHz, dept 135, C_6D_6): 127.98, 125.93, 125.08, 123.34, 90.09, 62.22, 60.52, 54.45, 54.39, 35.73, 35.61, 33.38, 33.17, 30.94, 30.85, 27.54, 27.48, 27.37, 27.26, 26.76; ^{31}P NMR (202 MHz, C_6D_6): 4.2.

3.1.3. Synthesis of Chloro(dicyclohexyl)(1,4-dimethoxy-3-phenylnaphthalen-2-yl) phosphonium chloride (**7**)

To the flame-dried Schlenk tube filled with argon 556 mg (1 mmol), **6** and 8 mL of absolute CPME (CPME could be replaced with DME) was added. The Schlenk tube was closed with a rubber septum and cooled down to 0 °C, and a solution of 400 mg of $C_2O_2Cl_2$ in 5 mL of toluene was slowly added via a septum. After 15 min of stirring at 0 °C, the reaction was allowed to warm up to ambient temperature and was stirred for the next 30 min. The progress of the reaction was controlled by ^{31}P NMR. ^{31}P NMR (202 MHz, D_2O capillary): 97.5. The reaction mixture quenched by water gave exclusively phosphine oxide **6**. ^{31}P NMR (202 MHz, D_2O capillary): 50.4.

3.1.4. Transformation of **7** to **5**

To a solution of **7** stirred at 0 °C, as presented above, the solution of 250 mg of anhydrous Li_2S in 10 mL of anhydrous acetonitrile (which could be replaced by DME) was added via a syringe. The reaction was allowed to warm up to ambient temperature and was left stirring for the next 16 h. Next, 100 mL of cold water was poured in. The crude product was extracted with dichloromethane 3 × 20 mL, the organic phase was separated and dried by magnesium sulfate, and product **5** was isolated by chromatography on a SiO_2 column using the hexane/acetone = 6/1 to 3/1 solvent mixtures to elute the substances. Yield 0.47 g (80%).

3.1.5. Transformation of **7** to Dicyclohexyl[1,4-dimethoxy-3-(2,4,6-trimethoxyphenyl) naphthalen-2-yl]phosphane borane **8**

To a solution of **7** stirred at 0 °C, as presented above, the solution of 3 mL of 2M $LiBH_4$ in THF was added via syringe. The reaction was allowed to warm up to ambient temperature and was stirred for the next 16 h. Next, 100 mL of cold water was poured in, the crude product was extracted with dichloromethane 3 × 20 mL, the organic phase was separated and dried by magnesium sulfate, and product **8** was isolated by chromatography on a SiO_2 column using the hexane/acetone = 6/1 to 3/1 solvent mixtures to elute the substances. Yield 0.5 g (90%). ^{1}H NMR (500 MHz, C_6D_6): 8.12 (m, 2H), 7.55 (m, 2H), 6.18 (s, 2H), 4.13 (s, 3H), 3. 87 (s, 3H), 3.66 (s, 6H), 3.55 (s, 3H), 2.50 (m, 2H), 1.89 (m, 2H), 1.79 (m, 2H), 1.60 (m, 4H), 1.42 (m, 4H), 1.24 (m, 8H), 0.01 (m, 3H); ^{31}P NMR (202 MHz, $CDCl_3$): 35.9; ^{11}B NMR (160 MHz, $CDCl_3$): 41.9.

3.1.6. Transformation of **7** to Dicyclohexyl[1,4-dimethoxy-3-(2,4,6-trimethoxyphenyl) naphthalen-2-yl]phosphane **1**

To a solution of **7** stirred at 0 °C**,** as presented above, 30 mmol of $LiAlH_4$ in 20 mL of DME (which could be replaced by CPME) was added via a syringe. The reaction was allowed to warm up to ambient temperature and stirred for the next 16 h. Next, the reaction mixture was cooled down to −15 °C, 30 mL of Et_2O was added followed by the addition of saturated solution of NH_4Cl. Next, 100 mL of cold water was poured in and the organic phase was separated and dried by magnesium sulfate. The solvent was evaporated under reduced pressure to furnish **1** in an quantitative yield and 98% purity. The product was purified chromatographically on a short and degassed SiO_2 flash column eluted with benzene to give 465 mg of **1** (85%).

3.1.7. Transformation of **8** to **1**

Approximately 564 mg **8** was dissolved in 5 mL of hydrazine and 5 mL of benzene mixture. The air in the vessel was replaced with argon. The vessel was sealed with a glass stopper, and the reaction mixture was stirred at 80 °C for 16 h. Next, the reaction mixture was cooled down to ambient temperature, and 100 mL of cold water was added. The product was extracted with 20 mL of E_2O, the organic phase was separated dried by magnesium sulfate, and solvents were evaporated under reduced pressure to yield 0.6 g (95%) of **1**.

3.1.8. Synthesis of Complex **9**

The mixture of 123 mg of **1**, 51 mg of $Pd(CH_3CN)_2Cl_2$ (the precursors $Pd(PhCN)_2Cl_2$ and $Pd(^t\text{-}BuCN)_2Cl_2$ could be used instead of $Pd(CH_3CN)_2Cl_2$ with a similar outcome for the reaction) and 3 mL of DCM was subjected to ultrasound irradiation for 1 h at 25 °C and left stirring for 16 h at ambient temperature. The solution was filtered through a 0.45 μm PTFE syringe filter. Solvents were evaporated under reduced pressure, and the obtained solid was crystalized from CH_3CN to yield 107 mg (74%) of **9** as an orange–brown crystalline powder. ^{1}H NMR (500 MHz, $CDCl_3$): 8.17 (m, 1H), 7.99 (m, 1H), 7.61 (m, 2H), 6.14 (s, 2H), 4.11 (s, 3H), 4. 09 (s, 3H), 3.76 (s, 6H), 3.49 (s, 3H), 3.00 (bq, J = 12.1, 2H), 2.34 (m, 2H), 1.91 (m, 4H), 1.80 (m, 6H), 1.68 (m, 2H), 1.28 (m, 6H); ^{13}C NMR (126 MHz, dept 135, $CDCl_3$): 127.75, 126.33, 123.70, 123.48, 92.89, 63.11, 61.80, 57.51, 56.07, 37.98, 37.76, 29.38, 29.23, 27.51, 27.40, 27.26, 27.16, 25.93. ^{31}P NMR (202 MHz, $CDCl_3$): 68.73. HPLC-MS (CH_3CN/H_2O = 80/20, 0.3 mL/min, rf 3.3 min): measured 701.1869 Da $[C_{34}H_{43}O_7PPd]^+$, calculated 701.1869 Da, which corresponds to the cation in which Cl^- is replaced with a formate anion from the one used as a mobile phase additive (formic acid).

3.1.9. Synthesis of Complex **10**

The reaction mixture of 246 mg of **1**, 51 mg of $Pd((CH_3)_3CCN)_2Cl_2$ and 3 mL of DCM. was subjected ultrasound irradiation for 1 h at 25 °C and left stirring for 24 h at 40 °C. The solution was filtered through a 0.45 μm PTFE syringe filter. Solvents were evaporated under

reduced pressure, and the obtained solid was crystalized from a mixture of DCM/Et_2O to yield 70 mg (30%) of **10** as an orange–brown crystalline powder. ^{1}H NMR (500 MHz, CD_2Cl_2): 8.36 (d, J = 8.2, 1H), 8.23 (d, J = 7.9, 1H), 8.20 (d, J = 7.9, 1H), 7.77 (m, 2H), 7.48 (t, J = 7.6, 1H), 7.35 (t, J = 7.6, 1H), 6.36 (s, 2H), 6.30 (s, 2H), 4.32 (s, 3H), 3.97 (s, 3H), 3.93 (s, 3H), 3.75 (s, 6H), 3.74 (s, 6H), 3.59 (s, 3H), 3.51 (s, 3H), 2.85 (m, 4H), 1.0–2.00 (m, 40H); ^{31}P NMR (202 MHz, CD_2Cl_2): 76.34 (MeP^+), 37.37 (PPd^-); HPLC-MS (CH_3CN/H_2O = 80/20, 0.3 mL/min, rf 2.7 min): measured 565.3065 Da $[C34H45O5P]^+$, calculated 565.3077 Da, and −721.1341 Da $[C_{33}H_{41}O_7PClPd]^-$, calculated −721.1319 Da which corresponds to the anion in which Cl^- is replaced with a formate anion from the one used as a mobile phase additive (formic acid).

3.1.10. Synthesis of Complex **11**

The reaction mixture of 50 mg of **10**, 50 mg of **1**, and 3 mL of DCM was subjected to ultrasound irradiation for 1 h at 25 °C and left stirring for 7 days at 40 °C. The solution was filtered through a 0.45 µm PTFE syringe filter. Solvents were evaporated under reduced pressure and obtained solid crystallized from a mixture of DCM/Et_2O to yield 27 mg (50%) of **11** as an orange–brown crystalline powder. HPLC-MS (CH_3CN/H_2O = 80/20, 0.3 mL/min, rf 2.5 min): measured 682.1926 Da $[C_{34}H_{43}NO_5PPd]^+$, calculated 682.1908 Da, and less intense 723.21 Da $[C_{36}H_{46}N_2O_5PPd]^+$, calculated 723.21 Da which corresponds to the cations in which Cl^- and the phosphine ligand were replaced under ESI conditions with one or two molecules of highly coordinating mobile phase (CH_3CN). ^{1}H NMR (500 MHz, CD_2Cl_2): 8.26 (d, J = 8.8, 1H), 8.15 (d, J = 8.2, 1H), 8.07 (d, J = 8.2, 1H), 7.85 (d, J = 8.2, 1H), 7.68 (d, J = 8.8, 1H), 7.56 (t, J = 8.2, 1H), 7.48 (m, 2H), 7.36 (t, J = 8.8, 2H), 7.27 (t, J = 7.6, 1H), 6.81 (t, J = 7.6, 1H), 6.36 (s, 1H), 6.30 (s, 2H), 6.28 (s, 1H), 4.40 (s, 3H), 3.98 (s, 3H), 3.94 (s, 3H), 3.93 (s, 3H), 3.79 (s, 3H), 3.76 (s, 3H), 3.73 (s, 6H), 3.65 (s, 3H), 3.59 (s, 3H), 3.58 (s, 3H), 3.54 (s, 3H), 3.45 (s, 3H), 1.00–2.50 (m, 100H). ^{31}P NMR (202 MHz, CD_2Cl_2): 64.05 (d, J_{pp} = 445.3, 1P), 31.53 (d, J_{pp} = 445.3, 1P).

3.1.11. Synthesis of Complex **12**

To the mixture of 100 mg in **5** and 2 mL of DCM, a solution of 33 mg of $Pd(PhCN)_2Cl_2$ in 2 mL of DCM was added. The reaction mixture was subjected to ultrasound irradiation for 1h at 25 °C. The solution was filtered through a 0.45 µm PTFE syringe filter. Solvents were evaporated under reduced pressure, and the obtained solid was crystalized from a mixture of DMC/Et_2O to yield 100 mg (76%) of **12** as an orange–brown crystalline powder. ^{1}H NMR (500 MHz, DMSO-d_6): 8.17 (d, J = 7.7, 1H), 8.00 (dd, J = 7.6, 1.1, 1H), 7.64 (m, 2H), 6.12 (s, 2H), 4.09 (s, 3H), 3. 82 (s, 3H), 3.53 (s, 6H), 3.42 (s, 3H), 2.63 (m, 2H), 1.72 (m, 4H), 1.59 (m, 6H), 1.31 (m, 6H), 1.10 (m, 4H); ^{13}C NMR (126 MHz, dept 135, DMSO-d_6): 128.13, 126.62, 124.33, 123.24, 90.38, 63.63, 60.91, 55.52, 55.21, 27.80, 27.21, 26.61, 26.50, 26.35, 26.24, 26.05. ^{31}P NMR (202 MHz, DMSO-d_6): 65.79. The MS spectrum of the complex dominates the signal of the free ligand 583.26 Da $[C_{33}H_{43}O_5PS^+H^+]$.

3.1.12. Synthesis of Complex **14**

Ligand **13** and its complex **14** were obtained as reported previously [3,19].

3.2. Crystallography

The monocrystals, used for X-ray diffraction analysis, were grown from the supersaturated solutions of the corresponding complexes, which were obtained as a result of the partial evaporation of solvent under reduced pressure at 40 °C, followed by cooling to ambient temperature in sealed vessels and storage for the necessary time. The diffraction intensities for the crystal of **9** were measured at 120 K, for **10** and **11** at room temperature, and for **12** at 100 K. Data were collected on a SuperNova Rigaku Oxford Diffraction diffractometer (CuKa radiation λ = 1.54184 Å) for **9** and on an Oxford Diffraction Xcalibur CCD diffractometer (MoKa radiation λ = 0.71073 Å) for **10**, **11,** and **12**. The ω scan technique was applied for data collection using programs CrysAlis CCD and CrysAlis Red [50] for

data collection, cell refinement, and data reduction. The structures were solved by direct methods using SHELXS-97 and refined by the full-matrix least-squares on F^2 using the SHELXL-97 [51] implemented in Olex2 [52]. Non-hydrogen atoms apart from the atoms of solvent molecules in **9**, **11,** and **12** were refined with anisotropic displacement parameters. The H atoms were positioned geometrically and were allowed to ride on their parent atoms, with U iso (H) = 1.2 U eq (C) and 1.5 for methyl groups. In **9** the diethyl ether and dichloromethane molecules are located at special positions around the twofold axis. **11** crystallizes as a dihydrate. The studied compounds are voluminous and the quality of the single crystals was low; however, it was possible to determine the crystal and molecular structures of each complex without any doubts.

Crystallographic data for **14** were reported previously [3].

4. Conclusions

The biaryl monophosphine-based transition metal catalysts belong to efficient and selective ones. The voluminous cyclohexyl substituents at the P atom are supposed to protect it from oxidation and enhance reductive elimination. On the other hand, the biaryl fragment provides the catalytical selectivity. To prevent the formation of palladacycles, the *ortho*-substituents at the biaryl moiety are frequently incorporated. Despite the large size of substituents at the phosphorous atom, this group of compounds exhibits a wide range of coordination behaviors which should be taken into consideration when designing new catalysts.

We have presented here an interesting example of a series of complexes based on a biaryl monophosphine ligand MeO*Sym*-Phos and its sulfide derivative MeO*Sym*-PhosS. Depending on the synthesis conditions, the ligand may form various complexes:

(i) Under mild conditions (35 °C), a C,P chelated Pd(II) complex of **9** is formed;
(ii) At a slightly higher temperature (40 °C), a by-product complex **10** is obtained through demethylation of one of the methoxy groups at the 1,4-dimethoxynaphthalene fragment;
(iii) **11** can serve as an example of an intermediate stage of P-methylation;
(iv) **12** is the first report on a palladium(II) coordination compound of biaryl monophosphine sulfide and shows monodentate S ligation.

It is worth noting that we also observed in two structures (**11** and **12**) a special molecular arrangement favoring C–H. . .Pd agostic interactions, which may be regarded as an important preactivation stage of the demethylation reaction. However, this problem requires further computational studies.

To summarize the knowledge on the coordination modes of biaryl monophosphine palladium complexes, we compared our experimental results with the structural data found in the CSD. This short literature review together with our experimental results shows that particular attention should be paid during the preparation of catalysts, since variation in the reaction conditions and small structural changes in the ligand core may lead to different complexes, which are not necessarily catalytically active or stable. The presented studies may be helpful in rationally designing new, efficient, and highly selective catalysts in the future.

Author Contributions: Conceptualization, O.M.D. and B.M.; methodology, B.M.; software, B.M., I.D. and R.J.; investigation, O.M.D., B.M., R.J. and I.D.; data curation, B.M.; writing—original draft preparation, B.M., O.M.D. and R.J.; writing—review and editing, B.M., O.M.D. and R.J.; visualization, B.M. and O.M.D. All authors have read and agreed to the published version of the manuscript.

Funding: The research was partially funded by financial support from the Polish National Science Centre, grant number 2019/33/B/NZ7/01608, and carried out with equipment purchased thanks to the financial support of the European Regional Development Fund in the framework of the Operational Program Development of Eastern Poland 2007–2013 (Contract No. POPW.01.03.00-06-009/11-00, equipping the laboratories of the Faculties of Biology and Biotechnology, Mathematics, Physics and Informatics, and Chemistry for studies of biologically active substances and environmen-

tal samples). This work was created as a part of a research internship at the Department of Organic Chemistry and Technology at Cracow University of Technology, Poland.

Conflicts of Interest: The authors declare no conflict of interest.

References

1. Dotta, P.; Kumar, P.G.A.; Pregosin, P.S.; Albinati, A.; Rizzato, S. Pd-(MOP) chemistry: Novel bonding modes and interesting charge distribution. *Organometallics* **2003**, *22*, 5345–5349. [CrossRef]
2. Demchuk, O.M.; Kaplon, K.; Mazur, L.; Strzelecka, D.; Pietrusiewicz, K.M. Readily available catalysts for demanding Suzuki-Miyaura couplings under mild conditions. *Tetrahedron* **2016**, *72*, 6668–6677. [CrossRef]
3. Demchuk, O.M.; Kielar, K.; Pietrusiewicz, K.M. Rational design of novel ligands for environmentally benign cross-coupling reactions. *Pure Appl. Chem.* **2011**, *83*, 633–644. [CrossRef]
4. Barder, T.E.; Walker, S.D.; Martinelli, J.R.; Buchwald, S.L. Catalysts for Suzuki-Miyaura coupling processes: Scope and studies of the effect of ligand structure. *J. Am. Chem. Soc.* **2005**, *127*, 4685–4696. [CrossRef]
5. Altman, R.A.; Buchwald, S.L. Pd-catalyzed Suzuki-Miyaura reactions of aryl halides using bulky biarylmonophosphine ligands. *Nat. Protoc.* **2007**, *2*, 3115–3121. [CrossRef] [PubMed]
6. Kaplon, K.; Frynas, S.; Miroslaw, B.; Lipkowski, J.; Demchuk, O.M. An Efficient Asymmetric Cross-Coupling Reaction in Aqueous Media Mediated by Chiral Chelating Mono Phosphane Atropisomeric Biaryl Ligand. *Catalysts* **2023**, *13*, 353. [CrossRef]
7. Demchuk, O.M.; Arlt, D.; Jasinski, R.; Pietrusiewicz, K.M. Relationship between structure and efficiency of atropisomeric phosphine ligands in homogeneous catalytic asymmetric hydrogenation. *J. Phys. Org. Chem.* **2012**, *25*, 1006–1011. [CrossRef]
8. Demchuk, O.M.; Martyna, A.; Kwasnik, M.; Szwaczko, K.; Strzelecka, D.; Miroslaw, B.; Pietrusiewicz, K.M.; Urbanczyk-Lipkowska, Z. A Modular Approach to Atropisomeric Bisphosphines of Diversified Electronic Density on Phosphorus Atoms. *Molecules* **2022**, *27*, 5504. [CrossRef]
9. Jasinski, R.; Demchuk, O.M.; Babyuk, D. A Quantum-Chemical DFT Approach to Elucidation of the Chirality Transfer Mechanism of the Enantioselective Suzuki-Miyaura Cross-Coupling Reaction. *J. Chem.* **2017**, *2017*, 3617527. [CrossRef]
10. Ruiz-Castillo, P.; Buchwald, S.L. Applications of Palladium-Catalyzed C-N Cross-Coupling Reactions. *Chem. Rev.* **2016**, *116*, 12564–12649. [CrossRef]
11. Singh, C.; Rathod, J.; Jha, V.; Panossian, A.; Kumar, P.; Leroux, F.R. Modular Synthesis of Biaryl-Substituted Phosphine Ligands: Application in Microwave-Assisted Palladium-Catalyzed C-N Cross-Coupling Reactions. *Eur. J. Org. Chem.* **2015**, *2015*, 6515–6525. [CrossRef]
12. Xu, J.; Liu, R.Y.; Yeung, C.S.; Buchwald, S.L. Monophosphine Ligands Promote Pd-Catalyzed C-S Cross-Coupling Reactions at Room Temperature with Soluble Bases. *ACS Catal.* **2019**, *9*, 6461–6466. [CrossRef] [PubMed]
13. Tabassum, S.; Zahoor, A.F.; Ahmad, S.; Noreen, R.; Khan, S.G.; Ahmad, H. Cross-coupling reactions towards the synthesis of natural products. *Mol. Divers.* **2022**, *26*, 647–689. [CrossRef] [PubMed]
14. Buskes, M.J.; Blanco, M.J. Impact of Cross-Coupling Reactions in Drug Discovery and Development. *Molecules* **2020**, *25*, 3493. [CrossRef]
15. Devendar, P.; Qu, R.Y.; Kang, W.M.; He, B.; Yang, G.F. Palladium-Catalyzed Cross-Coupling Reactions: A Powerful Tool for the Synthesis of Agrochemicals. *J. Agric. Food Chem.* **2018**, *66*, 8914–8934. [CrossRef]
16. Horbaczewskyj, C.S.; Fairlamb, I.J.S. Pd-Catalyzed Cross-Couplings: On the Importance of the Catalyst Quantity Descriptors, mol % and ppm. *Org. Process. Res. Dev.* **2022**, *26*, 2240–2269. [CrossRef]
17. McCarthy, S.; Braddock, D.C.; Wilton-Ely, J.D.E.T. Strategies for sustainable palladium catalysis. *Coord. Chem. Rev.* **2021**, *442*, 213925. [CrossRef]
18. Liu, J.; Chen, Z.X.; Liu, C.B.; Zhang, B.; Du, Y.H.; Liu, C.F.; Ma, L.; Xi, S.B.; Li, R.L.; Zhao, X.X.; et al. Molecular engineered palladium single atom catalysts with an M-C1N3 subunit for Suzuki coupling. *J. Mater. Chem. A* **2021**, *9*, 11427–11432. [CrossRef]
19. Demchuk, O.M.; Yoruk, B.; Blackburn, T.; Snieckus, V. A mixed naphthyl-phenyl phosphine ligand motif for Suzuki, Heck, and hydrodehalogenation reactions. *Synlett* **2006**, *2006*, 2908–2913. [CrossRef]
20. Groom, C.R.; Bruno, I.J.; Lightfoot, M.P.; Ward, S.C. The Cambridge Structural Database. *Acta Cryst.* **2016**, *B72*, 171–179. [CrossRef] [PubMed]
21. Demchuk, O.M.; Swierczynska, W.; Dziuba, K.; Frynas, S.; Flis, A.; Pietrusiewicz, K.M. Raney-Ni reduction of phosphine sulfides. *Phosphorus Sulfur Silicon Relat. Elem.* **2017**, *192*, 64–68. [CrossRef]
22. Dybala, I.; Demchuk, O.M. Tris(acetonitrile)chloropalladium tetrafluoroborate synthesis, application and structural analysis. *J. Mol. Struct.* **2016**, *1121*, 135–141. [CrossRef]
23. Sajjad, M.A.; Christensen, K.E.; Rees, N.H.; Schwerdtfeger, P.; Harrison, J.A.; Nielson, A.J. New complexity for aromatic ring agostic interactions. *Chem. Commun.* **2017**, *53*, 4187–4190. [CrossRef]
24. Lin, X.; Wu, W.; Mo, Y. Agostic Interactions in Early Transition-Metal Complexes: Roles of Hyperconjugation, Dispersion, and Steric Effect. *Chem. Eur. J.* **2019**, *25*, 6591. [CrossRef]
25. Brookhart, M.; Green, M.L.H.; Parkin, G. Agostic interactions in transition metal compounds. *Proc. Natl. Acad. Sci. USA* **2007**, *104*, 6908–6914. [CrossRef]

26. Braga, D.; Grepioni, F.; Biradha, K.; Desiraju, G.R. Agostic interactions in organometallic compounds. A Cambridge Structural Database study. *J. Chem. Soc. Dalton Trans.* **1996**, *20*, 3925–3930. [CrossRef]
27. Hupf, E.; Malaspina, L.A.; Holsten, S.; Kleemiss, F.; Edwards, A.J.; Price, J.R.; Kozich, V.; Heyne, K.; Mebs, S.; Grabowsky, S.; et al. Proximity Enforced Agostic Interactions Involving Closed-Shell Coinage Metal Ions. *Inorg. Chem.* **2019**, *58*, 16372–16378. [CrossRef]
28. Grubbs, R.H.; Coates, G.W. α-Agostic Interactions and Olefin Insertion in Metallocene Polymerization Catalysts. *Acc. Chem. Res.* **1996**, *29*, 85–93. [CrossRef]
29. Xu, C.; Li, G.; Etienne, M.; Leng, X.; Chen, Y. α-C–C agostic interactions and C–H bond activation in scandium cyclopropyl complexes. *Inorg. Chem. Front.* **2020**, *7*, 4822–4831. [CrossRef]
30. Moss, G.P.; Smith, P.A.S.; Tavernier, D. Glossary of class names of organic compounds and reactivity intermediates based on structure (IUPAC Recommendations 1995). *Pure Appl. Chem.* **1995**, *67*, 1307–1375. [CrossRef]
31. Salzer, A. Nomenclature of Organometallic Compounds of the Transition Elements. *Pure Appl. Chem.* **1999**, *71*, 1557–1585. [CrossRef]
32. Cook, T.R.; Stang, P.J. Recent Developments in the Preparation and Chemistry of Metallacycles and Metallacages via Coordination. *Chem. Rev.* **2015**, *115*, 7001–7045. [CrossRef] [PubMed]
33. Yin, C.; Du, J.; Olenyuk, B.; Stang, P.J.; Sun, Y. The Applications of Metallacycles and Metallacages. *Inorganics* **2023**, *11*, 54. [CrossRef]
34. Sun, Y.; Stang, P.J. Metallacycles, metallacages, and their aggregate/optical behavior. *Aggregate* **2021**, *2*, e94. [CrossRef]
35. Bosque, R.; Maseras, F. A theoretical assessment of the thermodynamic preferences in the cyclopalladation of amines. *Eur. J. Inorg. Chem.* **2005**, *2005*, 4040–4047. [CrossRef]
36. Montgomery, M.; O'Brien, H.M.; Mendez-Galvez, C.; Bromfield, C.R.; Roberts, J.P.M.; Winnicka, A.M.; Horner, A.; Elorriaga, D.; Sparkes, H.A.; Bedford, R.B. The surprisingly facile formation of Pd(i)-phosphido complexes from ortho-biphenylphosphines and palladium acetate. *Dalton Trans.* **2019**, *48*, 3539–3542. [CrossRef]
37. Allgeier, A.M.; Shaw, B.J.; Hwang, T.L.; Milne, J.E.; Tedrow, J.S.; Wilde, C.N. Characterization of Two Stable Degradants of Palladium (t)BuXPhos Catalyst and a Unique Dearomatization Reaction. *Organometallics* **2012**, *31*, 519–522. [CrossRef]
38. Christmann, U.; Pantazis, D.A.; Benet-Buchholz, J.; McGrady, J.E.; Maseras, F.; Vilar, R. Experimental and theoretical investigations of new dinuclear palladium complexes as precatalysts for the amination of aryl chlorides. *J. Am. Chem. Soc.* **2006**, *128*, 6376–6390. [CrossRef] [PubMed]
39. Toriumi, N.; Shimomaki, K.; Caner, J.; Murata, K.; Martin, R.; Iwasawa, N. Mechanistic Studies into Visible Light-Driven Carboxylation of Aryl Halides/Triflates by the Combined Use of Palladium and Photoredox Catalysts. *Bull. Chem. Soc. Jpn.* **2021**, *94*, 1846–1853. [CrossRef]
40. Lalloo, N.; Malapit, C.A.; Taimoory, S.M.; Brigham, C.E.; Sanford, M.S. Decarbonylative Fluoroalkylation at Palladium(II): From Fundamental Organometallic Studies to Catalysis. *J. Am. Chem. Soc.* **2021**, *143*, 18617–18625. [CrossRef]
41. Pratap, R.; Parrish, D.; Gunda, P.; Venkataraman, D.; Lakshman, M.K. Influence of Biaryl Phosphine Structure on C-N and C-C Bond Formation. *J. Am. Chem. Soc.* **2009**, *131*, 12240–12249. [CrossRef]
42. Shen, X.Q.; Jones, G.O.; Watson, D.A.; Bhayana, B.; Buchwald, S.L. Enantioselective Synthesis of Axially Chiral Biaryls by the Pd-Catalyzed Suzuki Miyaura Reaction: Substrate Scope and Quantum Mechanical Investigations. *J. Am. Chem. Soc.* **2010**, *132*, 11278–11287. [CrossRef] [PubMed]
43. Pan, F.; Boursalian, G.B.; Ritter, T. Palladium-Catalyzed Decarbonylative Difluoromethylation of Acid Chlorides at Room Temperature. *Angew. Chem.-Int. Ed.* **2018**, *57*, 16871–16876. [CrossRef] [PubMed]
44. Bruno, N.C.; Tudge, M.T.; Buchwald, S.L. Design and preparation of new palladium precatalysts for C-C and C-N cross-coupling reactions. *Chem. Sci.* **2013**, *4*, 916–920. [CrossRef] [PubMed]
45. Sivendran, N.; Pirkl, N.; Hu, Z.Y.; Doppiu, A.; Goossen, L.J. Halogen-Bridged Methylnaphthyl Palladium Dimers as Versatile Catalyst Precursors in Coupling Reactions. *Angew. Chem.-Int. Ed.* **2021**, *60*, 25151–25160. [CrossRef] [PubMed]
46. Biscoe, M.R.; Barder, T.E.; Buchwald, S.L. Electronic effects on the selectivity of Pd-catalyzed C-N bond-forming reactions using biarylphosphine ligands: The competitive roles of amine binding and acidity. *Angew. Chem.-Int. Ed.* **2007**, *46*, 7232–7235. [CrossRef] [PubMed]
47. Faller, J.W.; Wilt, J.C.; Parr, J. Kinetic resolution and unusual regioselectivity in palladium-catalyzed allylic alkylations with a chiral P,S ligand. *Org. Lett.* **2004**, *6*, 1301–1304. [CrossRef]
48. Faller, J.W.; Wilt, J.C. Palladium/BINAP(S)-catalyzed asymmetric allylic amination. *Org. Lett.* **2005**, *7*, 633–636. [CrossRef]
49. Gilbertson, S.R.; Wang, X.F. Synthesis of (dicyclohexylphosphino)serine, its incorporation into a dodecapeptide, and the coordination of rhodium. *J. Org. Chem.* **1996**, *61*, 434–435. [CrossRef]
50. Rigaku Oxford Diffraction Ltd. *Crysalis-Pro Software System*, Version 1.171.38.46; Rigaku Corporation Ltd.; Rigaku Oxford Diffraction Ltd.; Rigaku Corporation: Oxford, UK, 2016.

51. Sheldrick, G.M. Crystal structure refinement with SHELXL. *Acta. Cryst.* **2015**, *C71*, 3–8. [CrossRef]
52. Dolomanov, O.V.; Bourhis, L.J.; Gildea, R.J.; Howard, J.A.K.; Puschmann, H. OLEX2: A complete structure solution, refinement and analysis program. *J. Appl. Crystallogr.* **2009**, *42*, 339–341. [CrossRef]

Disclaimer/Publisher's Note: The statements, opinions and data contained in all publications are solely those of the individual author(s) and contributor(s) and not of MDPI and/or the editor(s). MDPI and/or the editor(s) disclaim responsibility for any injury to people or property resulting from any ideas, methods, instructions or products referred to in the content.